Soft Tissue Anchoring Performance, Biomechanical Properties, and Tissue Reaction of a New Hernia Mesh Engineered to Address Hernia Occurrence and Recurrence

Mohamad M. Ibrahim
Division of Plastic, Maxillofacial, and Oral Surgery,
Department of Surgery, Duke University Medical Center,
DUMC 3181,
Durham, NC 27710
e-mail: mohamed.ibrahim@duke.edu

Jason L. Green
Duke University School of Medicine,
487 Medical Science Research Building 1,
203 Research Drive,
Durham, NC 27710
e-mail: jlg71@duke.edu

Jeffrey Everitt
Department of Pathology,
Duke University Medical Center,
Durham, NC 27710
e-mail: jeffrey.everitt@duke.edu

David Ruppert
Division of Plastic and Reconstructive Surgery,
Department of Surgery,
Duke University Medical Center,
Durham, NC 27710
e-mail: david.ruppert@duke.edu

Richard Glisson
Department of Orthopaedic Surgery,
Duke University Medical Center,
Durham, NC 27710
e-mail: r.r.glisson@duke.edu

Frank Leopardi
Department of Surgery,
Duke University Medical Center,
Durham, NC 27710
e-mail: frank.leopardi@duke.edu

Thomas Risoli
Department of Biostatistics and Bioinformatics,
Duke University Medical Center,
Durham, NC 27710
e-mail: thomas.risoli.jr@duke.edu

Maragatha Kuchibhatla
Department of Biostatistics and Bioinformatics,
Duke University Medical Center,
Durham, NC 27710
e-mail: maragatha.kuchibhatla@duke.edu

Randall Reynolds
Division of Lab Animal Resources (DLAR),
Duke University School of Medicine,
Durham, NC 27710
e-mail: randall.reynolds@duke.edu

Howard Levinson[1]
Division of Plastic and Reconstructive Surgery,
Department of Surgery,
Duke University Medical Center,
Durham, NC 27710
e-mail: howard.levinson@duke.edu

One opportunity to reduce hernia occurrence and recurrence rates (currently estimated to be 30% at 10 years postoperatively) is by enhancing the ability of hernia meshes to anchor into tissue to prevent mesh migration, mesh contraction, and mesh tearing away from tissue. To address this, we developed a novel moderate-weight, macroporous, polypropylene mesh (termed the T-line mesh) with mesh extensions to optimize anchoring. We examined the physical properties, biomechanical performance, and biocompatibility of this novel mesh versus a predicate mesh anchored with #0-suture. The physical properties of the T-line mesh and predicate mesh were measured using American Society for Testing and Materials (ASTM) standards. Meshes were implanted into a swine hernia model and harvested after one day to determine anchoring strength of the meshes in the perioperative period. A separate group was implanted into a swine hernia model and harvested at 30 days and 90 days for semiquantitative histological analysis of biocompatibility. T-line mesh physical properties were similar to commonly used moderate-weight meshes in thickness and areal density. The T-line mesh outperformed the predicate mesh in all mechanical testing ($P < 0.05$). In the perioperative period, the T-line mesh was ∼275% stronger ($P < 0.001$) than the standard of care. Histological analysis of biocompatibility demonstrated no significant difference between the T-line mesh and predicate mesh ($P > 0.05$). The T-line mesh is a novel hernia mesh that outperforms a predicate mesh in mechanical and biomechanical performance testing while exhibiting similar biocompatibility. The T-line mesh has the potential to reduce hernia occurrence and recurrence caused by mechanical failure. [DOI: 10.1115/1.4043740]

1 Introduction

Suture application of hernia mesh at the time of ventral hernia repair or laparotomy closure in high risk patients versus suture closure alone reduces hernia occurrence and recurrence rates from ∼50 to 60% to ∼20% because the mesh holds the soft tissue together and disperses force away from the midline closure [1–8]. Despite the clear benefits of hernia mesh repair, there is still an opportunity to improve upon mesh design to further reduce ventral hernia repair failure rates below 20%. One way to achieve this goal is to improve mesh anchoring to tissue so the mesh will not migrate, contract, or pull away from tissue as a result of mechanical tension. The primary cause of mesh migration, contraction, or pulling away from tissue is overloading from intra-abdominal tension (e.g., coughing, ileus, and sneezing), lateral pull from the oblique muscles, and contraction from myofibroblasts and fibroblasts [9]. This is particularly relevant in the early postoperative period when mesh is at greatest risk of failure because

[1]Corresponding author.

Manuscript received December 27, 2018; final manuscript received April 24, 2019; published online September 20, 2019. Assoc. Editor: Yaling Liu.

bioincorporation (i.e., tissue ingrowth into the mesh) has not yet occurred and mesh anchoring is completely dependent upon the strength of the mesh, suture, and tissue interface [9]. There are several approaches to anchoring mesh to tissue, but sutures are the most common anchors and they often fail because they tear through tissue or mesh, they break, or their knots unravel [10–14].

Performance under tension is related to how closely the mechanical properties of the suture, mesh, tissue match to each other and it also relates to the ultimate tensile strength (UTS) of the suture, mesh, and tissue, where UTS is the maximum amount of stress that a material can withstand prior to failing [15,16]. The UTS of the suture, mesh, tissue materials, and anchor points should exceed 16 N/cm because this is considered to be the maximum amount of load experienced by the abdominal wall (clinical benchmark for success) [15,17–20]. The UTS of moderate and heavy-weight textiles in benchtop testing frequently exceed 16 N/cm, which is why they do not tear, but light-weight meshes have been known to tear [21]. Interestingly, the UTS of suture, mesh, and tissue anchor points often do not meet this 16 N/cm benchmark and as a result, suture tears through tissue or mesh from physiologic loads. The UTS of suture, mesh, and tissue anchor points is determined by patient factors including but not limited to, obesity, diabetes, smoking, collagen disorders, multiple operations, and steroids, and it is also determined by the suture, mesh, tissue anchor point area, since tension (σ) = force (F)/area (A). A larger anchor point area of the suture–tissue interface will distribute the force over more tissue, reducing the tissue's normal stress. The tissue's shear stress will then be directly reduced through the Cauchy stress–tensor relationship (tensor transformation law), thereby allowing the anchor point to support a higher force before dehiscing. This fundamental engineering principle is the rationale behind the design of the mesh suture [22], which has demonstrated early clinical success [23]. Hence, wider sutures distribute forces better than narrow sutures, akin to how snowshoes distribute the force allowing for walking on top of snow, whereas boots focus the force creating high shear stress resulting in failure and collapse of the snow underfoot. The concept of distributing soft tissue forces across broad areas is exactly why hand surgeons use durable, multistranded sutures to repair flexor tendons under tension [24].

To demonstrate the relationships between suture, mesh, tissue anchor point area, and UTS, we created a novel moderate-weight macroporous, polypropylene mesh as defined by the synthetic mesh classification system of Earle et al. [25]. This mesh is termed the T-line mesh and features mesh extensions that are 29 times (1.1 cm wide extensions) the cross-sectional area of #0 polypropylene suture (Fig. 1). The extensions have blunt needles (identical sized needles to #0 suture needles) swaged onto their ends so the extensions can be sewn into fascia to anchor the mesh, eliminating the need for polypropylene suture or alternative fixation devices to anchor the mesh. Physical and mechanical properties (thickness, pore area, areal density, extension interspace distance, extension width, suture retention strength, ball burst, tongue tear resistance, tensile strength, and extension tensile strength) of the T-line mesh and the predicate mesh to which it was compared were quantified. We then compared anchor point performance and mesh biocompatibility of the T-line mesh to a currently marketed polypropylene mesh secured to the fascia with #0 polypropylene suture in a swine hernia model. A single polypropylene predicate mesh was selected for comparison rather than multiple meshes because the anchoring mechanisms are common between all hernia meshes and the objective of this study was to investigate the novel anchoring system of the T-line mesh versus a hernia mesh made of the same material with similar structural design. Our investigation illustrates that the T-line mesh design could significantly improve mesh performance across multiple clinically relevant benchmarks, possesses equivalent biocompatibility to a predicate, and has the potential to reduce hernia recurrence and occurrence.

2 Materials and Methods

2.1 Animals. All animal procedures and housing were performed under protocols approved by the Institutional Animal Care and Use Committee (IACUC) of Duke University. Twenty-four female Yucatan pigs (11.5–19.5 kg) were used throughout the study (S&S Farms, Ramona, CA). Animals were randomized into three groups corresponding to three follow-up time points (days 1, 30, and 90). Animals were individually housed in standard caging/pens for pigs. They were maintained on LabDiet® Mini-Pig HF (High Fortification) Grower (5L80) feed at 2%–3% of animal's body weight daily.

2.2 Mesh Implants. The novel mesh implant was knitted and characterized by a medical textile manufacturer. The woven mesh was physically characterized according to American Society for Testing and Materials (ASTM) standards for areal density and mass (ASTM D3776), thickness (ASTM D1777), flat width and

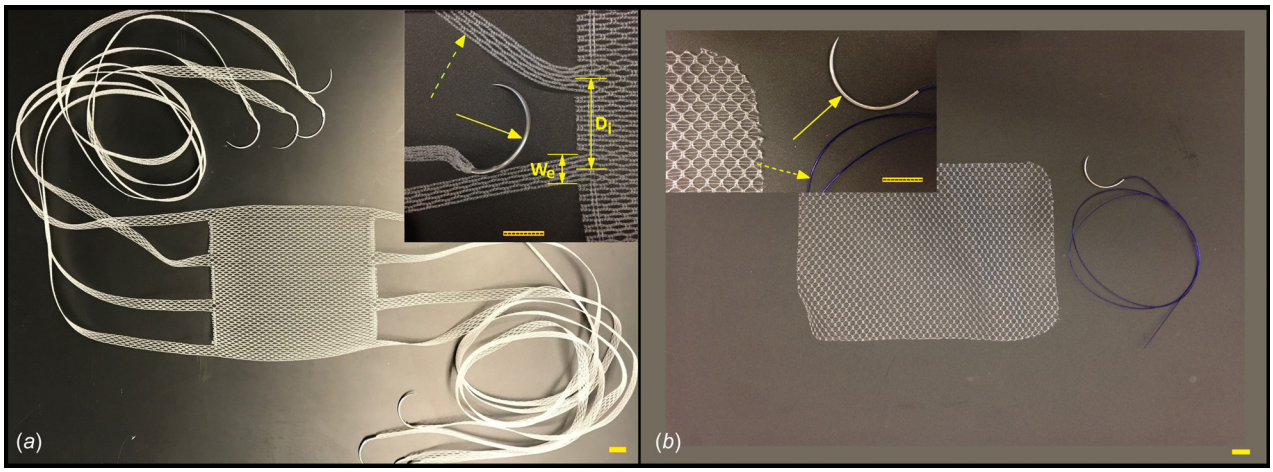

Fig. 1 T-line mesh and predicate control mesh: (*a*) the T-line mesh: extensions emanating from the body of the textile with Greishaber Spatula 21 (GS21) equivalent needles (inset) swaged on the ends of the extensions and (*b*) predicate polypropylene mesh and #0 prolene sutures with GS21 equivalent needles for anchoring mesh to fascia with interrupted stitches. The T-line mesh extensions increase surface area to distribute load when sutured into tissue relative to #0 polypropylene suture. Scale bar = 1 cm, solid arrow = GS-21 or equivalent needle, dashed arrow = extension/suture, D_i = 2 cm extension interspace distance shown here, and W_e = 0.6 cm extension width shown.

length (ASTM D3774), and pore size (internal testing method 8140). Mechanical performance of the woven mesh was evaluated according to standards for ball burst (ASTM D3787), tongue tear tensile strength (ASTM D2261), tensile strength and elongation (ASTM D5035), and suture retention (International Organization for Standardization (ISO) 7198). The predicate mesh for comparison was a Bard® Soft Mesh (Bard, Inc., Franklin Lakes, NJ).

2.3 Animal Surgical Preparation and Medication. Animals were fasted for approximately twelve hours prior to surgery. Animals were sedated with ketamine hydrochloride (22 mg/kg, intramuscular (IM)) and acepromazine (1.1 mg/kg, IM) with the use of isoflurane (1%–4%) via face mask and then intubated under anesthesia with 3% isoflurane inhalant to effect. The abdomen was shaved with a clipper and cleaned with chlorhexidine scrub and 70% isopropyl alcohol solution.

Preoperative analgesia consisted of buprenorphine (0.005 mg/kg, IM), and bupivacaine (1.0 mg/kg, infiltrated at incision site). Enrofloxacin (5.0 mg/kg, IM) was given pre-operatively for infection prophylaxis and continued per oral five days postoperatively. Midazolam (0.1 mg/kg, IM) and acepromazine (0.2 mg/kg, IM) was given immediately after extubation. Buprenorphine sustained release (0.02 mg/kg, subcutaneous) was given two hours after extubation. An additional option for analgesia was baytril (5 mg/kg, per oral) mixed with food for 5 days postoperatively.

2.4 Mesh Implantation for Biomechanical Analysis. A 20 cm midline ventral incision was made through the skin and subcutaneous fat exposing the midline fascia of the abdominal wall. The skin and fat were undermined bilaterally in a plane above the fascia for 12 cm lateral to the midline. The fascia was opened along the linea alba in the cranial–caudal direction for 15 cm and then closed using #0 polydioxanone (PDS) (Ethicon, Somerville, NJ) in an interrupted fashion with the suture bites spaced 1 cm lateral from the fascia wound edge and 1 cm apart in cranial–caudal direction. A four-extension, 10 cm long (coronal plane) × 10 cm wide (transverse plane) experimental mesh (T-line) or 10 cm square predicate mesh was randomized to either the caudal or rostral aspect of the fascia as an onlay. The other 5 cm portion of the fascia served as a sham control. An onlay approach was chosen because it is commonly used in hernia surgery; surgeons feel it is easier and faster than other surgical approaches (e.g., retrorectus and sublay); and onlay is sufficient to test the concept of anchoring strength and safety. All four extensions of the T-line mesh (1.1 cm wide extensions were spaced 2 cm on-center for a total of four extensions per each side) were placed in the external oblique aponeurosis and anterior rectus sheath fascia laterally (Fig. 2). The predicate mesh was cut to 10 × 10 cm dimensions from a 15 × 15 cm mesh leaving only two cut edges. The predicate mesh was anchored on each side with four #0 polypropylene sutures (Ethicon) (Fig. 2). The subcutaneous tissue was closed with 2-0 PDS in a continuous pattern. The deep dermis was approximated using 2-0 PDS in a continuous pattern, followed by dermal glue (Ethicon) to close the skin.

2.5 Mesh Implantation for Bio-Incorporation Analysis. A 15 cm midline ventral incision was made through the skin and subcutaneous fat exposing the midline fascia of the abdominal wall. The skin and fat were undermined bilaterally in a plane above the fascia for 12 cm lateral to the midline. The fascia was opened along the linea alba in the cranial–caudal direction for 10 cm and then closed using #0 polypropylene suture (Ethicon) in an interrupted fashion with the suture bites spaced 1 cm lateral from the fascia wound edge and 1 cm apart in cranial–caudal direction. A three-extension, 5 cm long (coronal plane) × 5 cm wide (transverse plane) experimental mesh (T-line) or a 5 cm long (coronal plane) × 10 cm wide (transverse plane) predicate mesh was randomized to either the caudal or rostral aspect of the fascia as an onlay (Figs. 2(*a*) and 2(*b*)). The other 5 cm portion of the fascia served as a sham control. All extensions of the T-line mesh

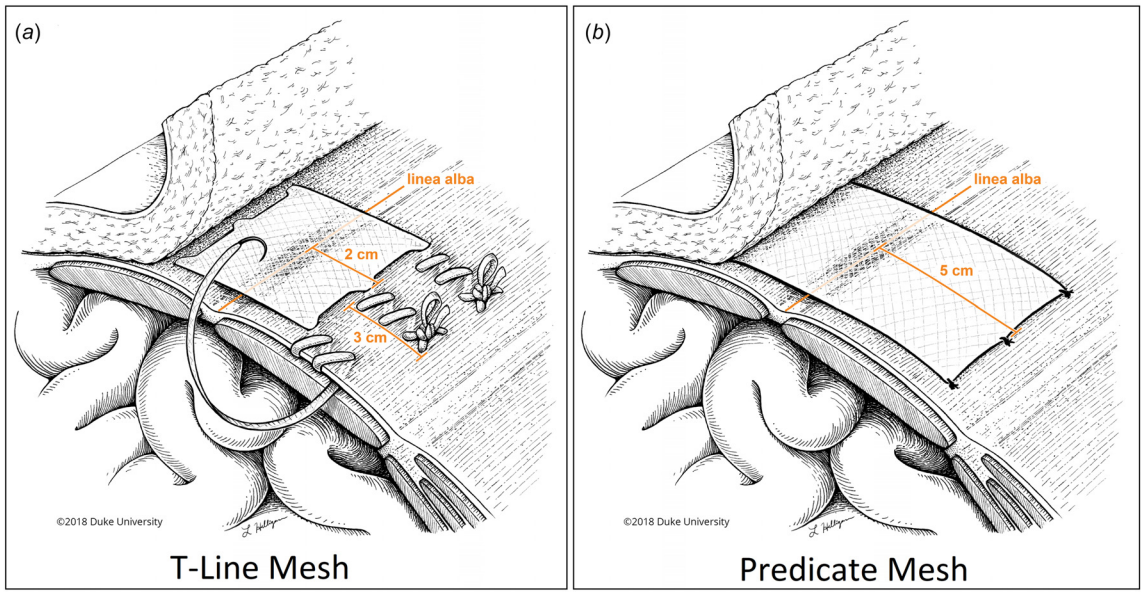

Fig. 2 Application techniques for onlay placement: (*a*) T-line mesh placement, the body extends 2 cm beyond the fascia incision, on either side of the incision, for adequate overlap onto healthy fascia. The extensions are then sewn into the fascia in a continuous, three-throw, locking stitch pattern (continuous running stitch pattern shown), for an additional 3 cm, so that the mesh body and extensions together add up to 5 cm of length away from the fascia incision. A loop-on-end surgeon knot followed by three throws is created at the end of each extension and (*b*) the predicate mesh is placed directly over the incision and the body of the textile extends 5 cm beyond the fascia incision on either side of the incision and is then secured with #0 polypropylene suture along the edge in a simple interrupted fashion. Sutures are placed at the corners of the mesh and then evenly spaced ~2 cm along the cephalocaudal length. Forty percent less T-line mesh textile is needed than the predicate mesh textile. The T-line mesh and control mesh were each implanted in four pigs for a total of eight pigs. Meshes were harvested on postoperative day 1 for mechanical analysis: (*a*) T-line mesh and (*b*) predicate mesh.

were placed in the external oblique aponeurosis and anterior rectus sheath fascia laterally as described in Fig. 2. The predicate mesh was anchored on each side as described in Fig. 2. The subcutaneous tissue was closed with 2-0 PDS in a continuous pattern. The deep dermis was approximated using 2-0 PDS in a continuous pattern, followed by dermal glue (Ethicon) to close the skin. Based on seroma formation seen in Sec. 2.4, a compression bandage was placed around the pig's trunk postoperatively to reduce seroma formation. Bandages were assessed daily for structural integrity and the surgical site was assessed under the bandage under light sedation. The bandages were removed once the seroma resolved. Cage side observations occurred daily on all animals. The frequency of observations increased if the animal was approaching a condition where pain or distress occurred.

2.6 Necropsy and Mesh Harvest. Animals were euthanized on days 1, 30, and 90 postimplantation ($N = 8$ for each time point, $N = 4$ mesh type per time point) via overdose of intravenous (auricular) barbiturate and were necropsied immediately following euthanasia. Two lateral and two horizontal incisions were made to remove en bloc the entire ventral wall containing the T-line mesh or predicate mesh. The implantation sites were grossly observed for signs of mesh or tissue tear or abnormal pathology. Following harvest of the ventral abdominal body wall and regional lymph nodes, a complete necropsy was performed on each animal with all body cavities and organs carefully examined in situ for the presence of lesions including evidence of infection or thrombosis.

2.7 Pathology Evaluation and Analyses (Inflammation, Bio-Incorporation and Fibrosis of the T-Line and the Predicate Mesh). Three 1×1 cm sections of body wall were cut perpendicular to the mesh in predesignated areas of both the T-line and predicate meshes from both peripheral as well as central regions of the mesh. In animals with the T-line mesh, three sites were sampled from areas of body wall with mesh extensions in addition to the central and peripheral mesh areas. Three body wall samples were also harvested from predesignated areas along the sham control site of the ventral abdominal incision. All tissue samples were fixed in 10% neutral buffered formalin for a minimum of 72 h at room temperature, embedded in paraffin, sectioned by microtomy at 5 μm, stained with hematoxylin and eosin (H&E), and examined by the pathologist. Slides were not examined in a "masked" manner by the pathologist since the mesh fibers have slightly different appearances making masking impossible. A semiquantitative histological scoring of the cellular reaction to the meshes was conducted on the H&E stained sections at 200× magnification (inflammation parameters at 400×) using modification of previously published scoring system [26] assessing inflammation, bio-incorporation, and fibrosis as defined in Table 1. Scores were assigned to each of the component parameters in five nonoverlapping fields per histological section along the entire mesh–tissue interface and then averaged.

2.8 Biomechanical Analysis in the Perioperative Period. To assess the biomechanical performance of the T-line mesh and the predicate mesh in the perioperative period when anchor point strength is needed most, meshes were harvested on postoperative day one ($N = 4$ for each mesh type) and assessed by uniaxial biomechanical testing. Briefly, each mesh was divided transversely at the midpoint of the mesh and 5 cm past the end of each extension for the T-line mesh or the edge of predicate mesh. The two parts of the mesh were categorized as cranial and caudal, respectively. Each respective section was secured in custom tissue grips to the actuator and table of a servohydraulic materials testing machine (model 1321, Instron Corp., Norwood, MA) (Fig. 3) and tested at a distraction rate of 100 mm/minute. Load and displacement were recorded at a sampling rate of 100 Hz. From this testing, a force (N) – displacement (mm) curve was generated and peak load to failure (N) recorded. The peak load to failure of each mesh was also normalized as a function of the cephalocaudal mesh length (N/cm) as indicated in Fig. 4(*a*). Specimen testing was filmed to document failure mode. Eight samples of T-line mesh and eight samples predicate mesh were tested.

2.9 Statistical Analysis. Perioperative biomechanical performance was analyzed using a two-way analysis of variance with Holm–Sidak posthoc mean comparison testing for implant type

Table 1 Semiquantitative histological modified scoring parameters for cellular reaction to implanted mesh.

	Score	0	1	2	3	4
Inflammation	PMNs	0/HPF	1–5/HPF	6–10/HPF	Marked (>10/HPF)	Abundant
	Lymphocytes/plasma cells	0/HPF	1–5/HPF	6–10/HPF	Marked (>10/HPF)	Abundant
	Macrophages	0/HPF	1–5/HPF	6–10/HPF	Marked (>10/HPF)	Abundant
	Foreign body giant cells	0/HPF	1–2/HPF	3–5/HPF	Marked (>5/HPF)	Abundant
	Necrosis	None	Minimal (0–25% field)	Mild (26–50% field)	Moderate 51–75% field)	Marked (>75% field)
Bioincorporation	Cell predominance	0% fibroblasts and 100% inflammatory cells	<25% fibroblasts and >75% inflammatory cells	>50% fibroblasts and <50% inflammatory cells	100% fibroblasts and 0% inflammatory cells	
	Cell infiltration	No cells in contact with mesh	Cells on periphery of mesh	Cells infiltrate into pores but not into center of the mesh	Cells infiltrate into pores and reach center of the mesh	
	Host extracellular matrix deposition	No host ECM	Host ECM deposited at the periphery of the mesh	Host ECM deposited around individual fibers but not bridging across interstices	Host ECM deposited within interstices and bridging across fibers	
	Neovascularization	No blood vessels present	Vessels only present at periphery not in interstices	Vessels present within interstices not bridging	Vessels bridging interstices of mesh	
	Fibrosis	Scar plate fully embedding entire mesh	Fibrosis surrounding individual mesh fibers and bridging in some places	Fibrosis surrounding individual mesh fibers but not bridging interstices	No fibrosis	

HPF = 400× high powered field. ECM = extracellular matrix.

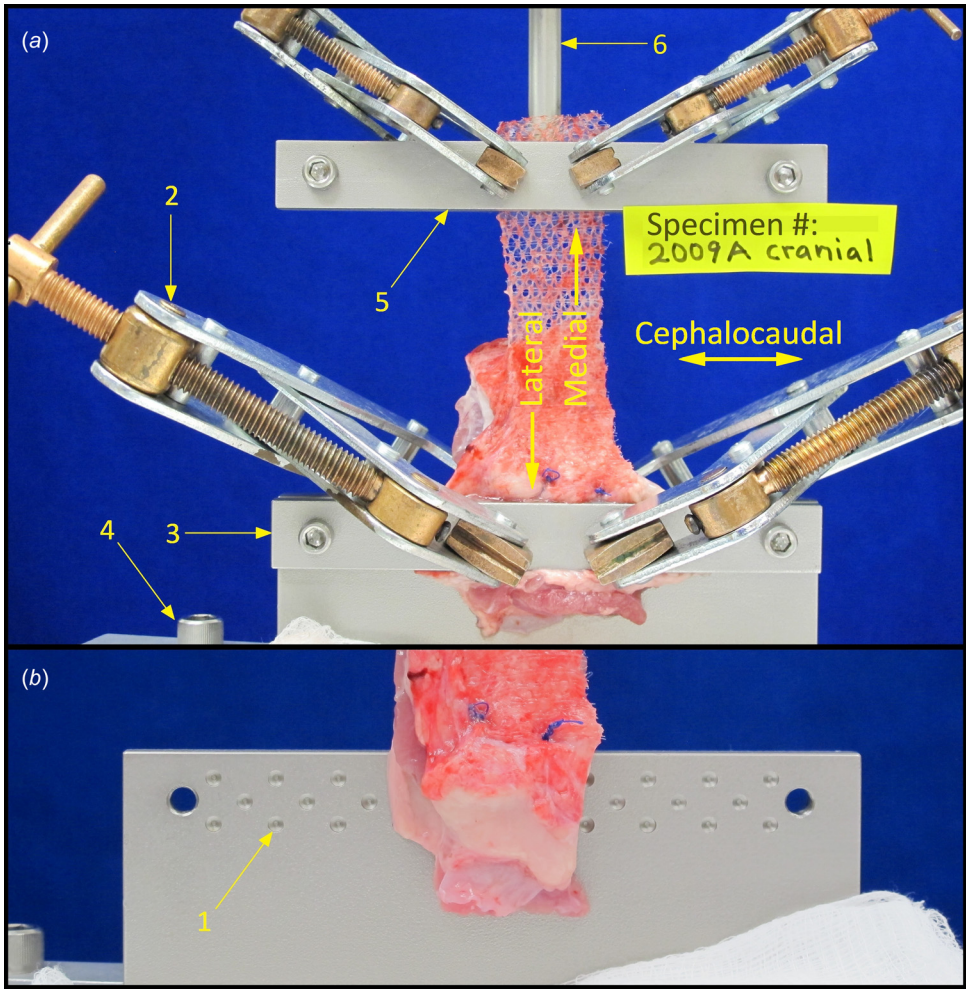

Fig. 3 Custom tissue grips comprised of opposing dimpled stainless-steel plates (1) bolted together. Clamps (2) were then applied over the specimen region to increase normal force and prevent tissue slipping within the grips. The lower grips (3) were bolted to the testing machine's table, (4) while the upper grips (5) were attached to the actuator-mounted load cell through a connecting rod (6). (*a*) Tissue specimen secured in upper and lower grips and (*b*) lower grip with tissue specimen prior to securing opposing grip.

and location of day one measures (peak load to failure) using a statistical analysis program (SIGMAPLOT v11.0, Systat Software Inc., San Jose, CA).

Continuous outcomes for bioincorporation, fibrosis, inflammation, and polymorphonuclear cells were summarized by means and standard deviations, while counts and percent were summarized categorical variables. Statistical analyses were performed comparing these outcomes at one month and three months between the treatment groups: T-line mesh and predicate mesh. Outcomes and change in each outcome were modeled using *t*-tests if the outcomes were normal or Wilcoxon tests if the outcomes were non-normal. Significance of the results was assessed without adjustment for multiple tests at alpha = 0.05, as well as with adjustment for multiple tests using Bonferroni correction. Analysis was conducted using SAS 9.4 (SAS Institute Inc., Cary, NC).

3 Results

The T-line mesh has properties akin to other commonly used moderate-weight meshes such as thickness (0.55 ± 0.01 mm) and areal density (90.40 ± 0.50 g/m^2), but also contains very large pores (2.82 ± 0.19 mm^2) which are typically only observed in light-weight meshes (Table 2) [27]. Furthermore, the T-line mesh possesses physical characteristics unique to its novel design—including extension width of 11 mm and extension interspace distance of 20 mm (Fig. 1). Mechanical characterization revealed the T-line mesh outperformed the predicate mesh in all tested variables and it also outperformed #0 polypropylene suture in tensile strength (Table 3).

3.1 Biomechanical Analysis in the Perioperative Period.

The peak load to failure 1 day postoperatively for T-line mesh (26.9 ± 10.9 N/mm) was ~275% greater ($P < 0.001$) than the standard of care (SOC) (9.8 ± 2.7 N/mm) ($N = 4$ for each mesh type) (Figs. 4(*a*) and 4(*b*)). The failure modes of both meshes were analyzed and the T-line mesh consistently failed (100%) by extensions pulling out of fascia, while the predicate mesh failed by either a single suture pulling out of fascia and mesh (62%) or both sutures pulling out of the mesh (39%) (Fig. 4(*c*)).

3.2 Necropsy and Mesh Harvest Observations

3.2.1 Macroscopic Findings 30 Days Postimplant Necropsy. There were no significant macroscopic findings in visceral organs of any of the eight pigs necropsied 30 days postimplant, and there was no gross indication of infection or fluid accumulation in the body cavities (abdominal or thoracic). No inguinal or axillary lymphadenomegaly or lesions were present. A minor area (2 cm) of omental adhesion was noted attached to the linea alba of one animal that had a T-line mesh. An animal with a predicate mesh

(*a*)

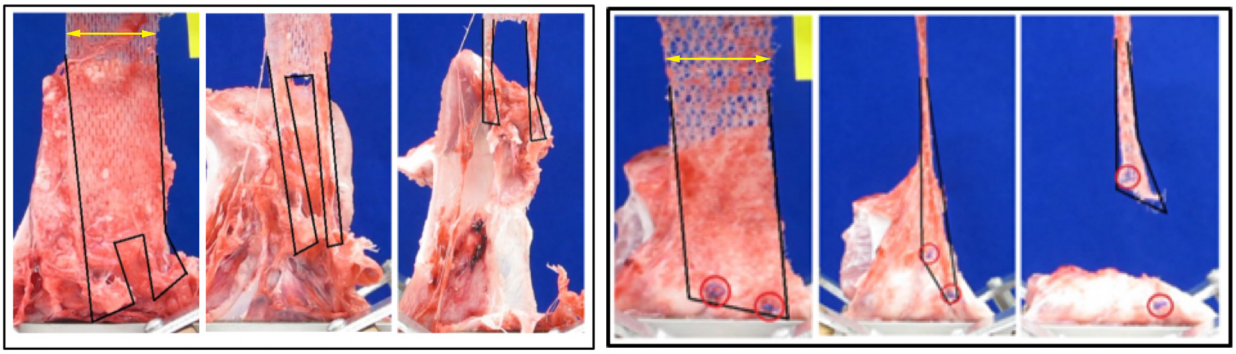

(*b*)

	T-Line Peak Load (N/cm)	
	Cranial	Caudal
2011A	12.4	40.8
2012A	18.5	38.8
2013A	37.1	23.3
2014A	17.1	27.3
mean	26.9	
St. Dev.	10.9	

	Predicate Peak Load (N/cm)	
	Cranial	Caudal
2009A	14.2	6.2
2010A	8.2	10.0
2015A	12.5	8.2
2016A	7.9	11.1
mean	9.8	
St. Dev.	2.7	

(*c*)

Failure Mode	T-Line	Predicate
Both anchor failures at anchor/mesh interface	0.0%	37.5%
1 Anchor failure at anchor/mesh interface & 1 Anchor failure at anchor/tissue interface	0.0%	62.5%
Failure of tissue remote to anchors	100.0%	0.0%

Fig. 4 Perioperative mechanical analysis: The experimental mesh and control mesh were each implanted in four pigs for a total of eight pigs. All meshes were harvested on postoperative day 1 for mechanical analysis. (*a*) Gross images of representative samples during the peak tensile load mechanical testing for T-line mesh (left) and predicate mesh (right). Meshes are outlined in black, the standard of care #0 sutures are outlined with the red circles, (*b*)The T-line mesh was ~275% stronger per unit length ($P < 0.001$) than the standard of care on peak load performance with no significant difference between cranial and caudal locations and (*c*) failure modes; the T-line mesh demonstrated one failure mode—pulling of the extensions out of fascia—while the predicate control mesh demonstrated two failure modes—one suture pulling out of fascia and the other out of mesh, and in the second failure mode, both sutures pulled out of the mesh. In first and fourth frames of *a* indicate cephalocaudal length of mesh as implanted in swine.

Table 2 T-line mesh physical characteristics (mean ± SD)

Dimension	T-line mesh	Predicate mesh	Predicate suture
Thickness (mm)	0.55 ± 0.01	0.50 ± 0.01	NA
Pore area (mm^2)	2.82 ± 0.19	0.56 ± 0.06	NA
Areal density (g/m^2)	90.40 ± 0.50	36.80 ± 0.35	NA
Extension interspace distance (center to center of extensions: cm)	2	NA	~2[a]
Extension width (mm)	11	NA	0.35–0.399[b]
Needle size	GS21 equivalent	NA	GS21

[a]Approximate spacing between simple interrupted stitches.
[b]Suture diameter per U.S. Pharmacopeia standard 861.

Table 3 Benchtop mechanical performance of T-line mesh (mean ± SD)

	T-line mesh	Predicate mesh	Predicate suture
Suture retention strength (N)[a]	26.09 ± 5.24	9.15 ± 3.72	NA
Ball burst (N)[b]	474.41 ± 23.75	233.92 ± 15.38	NA
Tongue tear resistance (N)	14.46 ± 1.74	11.71 ± 0.61	NA
Tensile strength (N)[c]	691.93 ± 73.48	111.92 ± 7.50	NA
Extension tensile strength (N)	217.39 ± 6.87	NA	50.46 ± 0.60

[a]Suture placed 2 mm from edge of textile per ISO 7198.
[b]Per 2.54 cm diameter steel ball rod according to ASTM D3787.
[c]Per 5 cm wide test specimens according to ASTM D5035.

had a small (1.5 cm) incisional separation in the area of the sham site that the omentum herniated through. There was no incarcerated gastrointestinal tissue tissue or necrotic omentum noted. In both T-line and predicate meshes, the tissue mesh interface was devoid of overt inflammation or necrosis. Both meshes were difficult to discern and to dissect due to incorporation into body wall layers. No macroscopic differences were noted between meshes. Adipose tissue and connective tissue were present at the tissue mesh interfaces and meshes were incorporated into the body wall. The pathologist was unable to dissect the mesh from body wall without causing marked artifact of the preparation and thus only limited attempts were made to fully discern the mesh. No displacement of either surgical mesh was noted.

3.2.2 Macroscopic Findings 90 Days Postimplant Necropsy. There were no significant macroscopic findings in visceral organs of the eight pigs necropsied 90 days postimplantation of mesh and there was no gross indication of infection or fluid accumulation in the abdominal cavities. No inguinal or axillary lymphadenomegaly or lesions were present. A small focal area (2 cm) of omental adhesion was noted adjacent to the linea alba in two predicate mesh animals and one T-line mesh animals, similar to the omental adhesions found at 30 days postoperatively. One pig with a T-line mesh had a fibrous adhesion from a section of jejunum to a location lateral to the linea alba and resting over a firm mass that was a knot associated with one of the lateral extensions of the T-line mesh. The surface of the body cavity was contracted and scarred, but there was no evidence of visible penetration of the mesh through the body wall. The pathologist noted that both the T-line and predicate meshes had more incorporation into connective tissue and body wall than at 30 days postoperatively. There was no macroscopic evidence of discoloration or suppuration and no indication of inflammation and/or infection. All tissues interfacing with mesh appeared to be adipose tissue or connective tissue and appeared white unless the interfacing tissue was muscle. As expected, at the 90-day time point, there was more contraction of both mesh types than at the 30 day. All T-line meshes appeared in their site of application. In one predicate mesh animal, the mesh contracted and migrated from its original location forming a firm ball of mesh at the rostral end of the surgical incision.

3.3 Histopathology Changes of Inflammation, Bioincorporation, and Fibrosis. Collectively, for 30 and 90 days postpredicate mesh implantation, microscopic changes were similar in all pigs within the group. Consistency of lesions was also found in the group of animals that had T-line meshes implanted. Semiquantitative scoring of inflammation (polymorphonuclear leukocytes, lymphocytes, and plasma cells, macrophages, and foreign-body giant cells) revealed similar findings in animals bearing either the predicate or T-line surgical meshes (Fig. 5). All animals had inflammatory responses typical of a foreign body reaction characterized by a moderate severity of pleocellular infiltrate consisting of large macrophages with numerous admixed polymorphonuclear leukocytes, lymphocytes, plasma cells, and multinucleated giant cells. In addition to the infiltration of inflammatory cells that comprised the predominant cellular reaction, there was substantial mesenchymal ingrowth (neovascularization, extracellular matrix (ECM) deposition, and fibrosis) representing bio-incorporation of the meshes corroborating what was noted macroscopically. Inflammation diminished from 30 to 90 days postoperatively (day 30 scores: 17 in T-line, 16 in predicate and day 90 scores: 10 in T-line mesh, 9 in predicate mesh), bioincorporation increased (day 30 scores: eight in T-line, seven in predicate and day 90 scores: nine in T-line mesh, ten in predicate mesh), and fibrosis decreased (day 30 scores: two in T-line, two in predicate and day 90 scores: 1.5 in T-line mesh, 1.5 in predicate mesh). In general, across the animals implanted with each mesh type, inflammation and mesenchymal infiltration were qualitatively and quantitatively similar as a function of time. There was no suppuration noted in specimens. Necrotic changes were minimal to mild and isolated to areas of inflammatory foreign body reaction.

4 Discussion

For a hernia repair to be effective and durable (resisting mesh contraction, migration, and mesh tearing away from tissue), it is proposed that the suture, mesh, tissue anchor points need to overcome four common failure modes: suture breaking, suture knot unraveling, suture tearing through mesh, and suture tearing through tissue at 16 N/cm of stress. In previous publications, we demonstrated a modified mesh design that leads to improved device performance [28]. Our earlier work compared the physical and mechanical properties of a crude version of the novel hernia mesh design to SOC suture and mesh using ASTM standards. In the earlier study, we utilized an ex vivo swine hernia benchtop model to illustrate how novel mesh anchor points are mechanically superior to a standard mesh secured with suture and we characterized the strength of different anchoring application techniques. This work established the basis for the development of the commercially viable version of T-line mesh reported in this study.

The novel T-line mesh was manufactured from polypropylene. We used polypropylene because it is commonly used in most current SOC meshes, is familiar to most surgeons, and its safety and biocompatibility profiles are well characterized. Of course, the T-line mesh could be manufactured from other filament materials such as polyester, polyvinylidene fluoride, or synthetic degradable yarns, if desired in the future. The T-line mesh is a macroporous, moderate-weight mesh as defined by the synthetic mesh classification system of Earle et al. [25] that meets all Food and Drug Administration (FDA) standards and outperforms a predicate mesh in all mechanical performance tests (Tables 2 and 3). We chose to create a macroporous, moderate-weight design because we wanted to use the least amount of mesh material in manufacturing the mesh (to reduce the likelihood of infection and prevent granuloma bridging) while maximizing mesh strength (preventing mesh tearing).

We assessed the biomechanical anchoring strength of the T-line mesh in comparison with a predicate mesh 1 day after mesh implantation. The immediate perioperative period is a time when anchor points are particularly susceptible to failure because of high tissue tension from edema and ileus, tissue enzyme elevation from surgery, and nascent bio-incorporation. Indeed, perioperative anchor point success determines long-term repair durability [29–31]. In this fragile time period, the T-line mesh was noted to be 275% stronger than SOC, reaching a supraphysiologic anchoring strength [17]. Creating supraphysiologic anchoring is critical to maintaining the biomechanical integrity of the abdominal wall and preventing hernia recurrence and occurrence. Interestingly, we also observed that when the T-line and predicate meshes were pulled to failure, the predicate mesh failed by suture tearing through mesh or tissue, whereas the T-line mesh failed through the extension tearing through tissue alone. Indicating the mesh-suture interface is significantly enhanced in the T-line mesh design. By reducing the mesh body width and using the extension to anchor into healthy fascia, forty percent less T-patented textile is needed than the predicate textile.

In addition to biomechanical performance, we analyzed local tissue reaction of the T-line mesh versus a predicate mesh by implanting both meshes in swine for 30 and 90 days and evaluating inflammation, bio-incorporation, and fibrosis. Local tissue reactivity, ISO 10993-6, is an important safety component for FDA class II hernia mesh devices. Overall there were no significant differences in inflammation, bio-incorporation, and fibrosis between the T-line mesh and predicate mesh, illustrating equivalent safety. The lack of differences between the meshes is not surprising given that both meshes are made from polypropylene. One predicate mesh contracted and migrated from its original location, which we contribute to insufficient anchor point fixation. The T-line mesh did not exhibit contraction or migration, but one knot was associated with an intestinal adhesion. The knot may have led

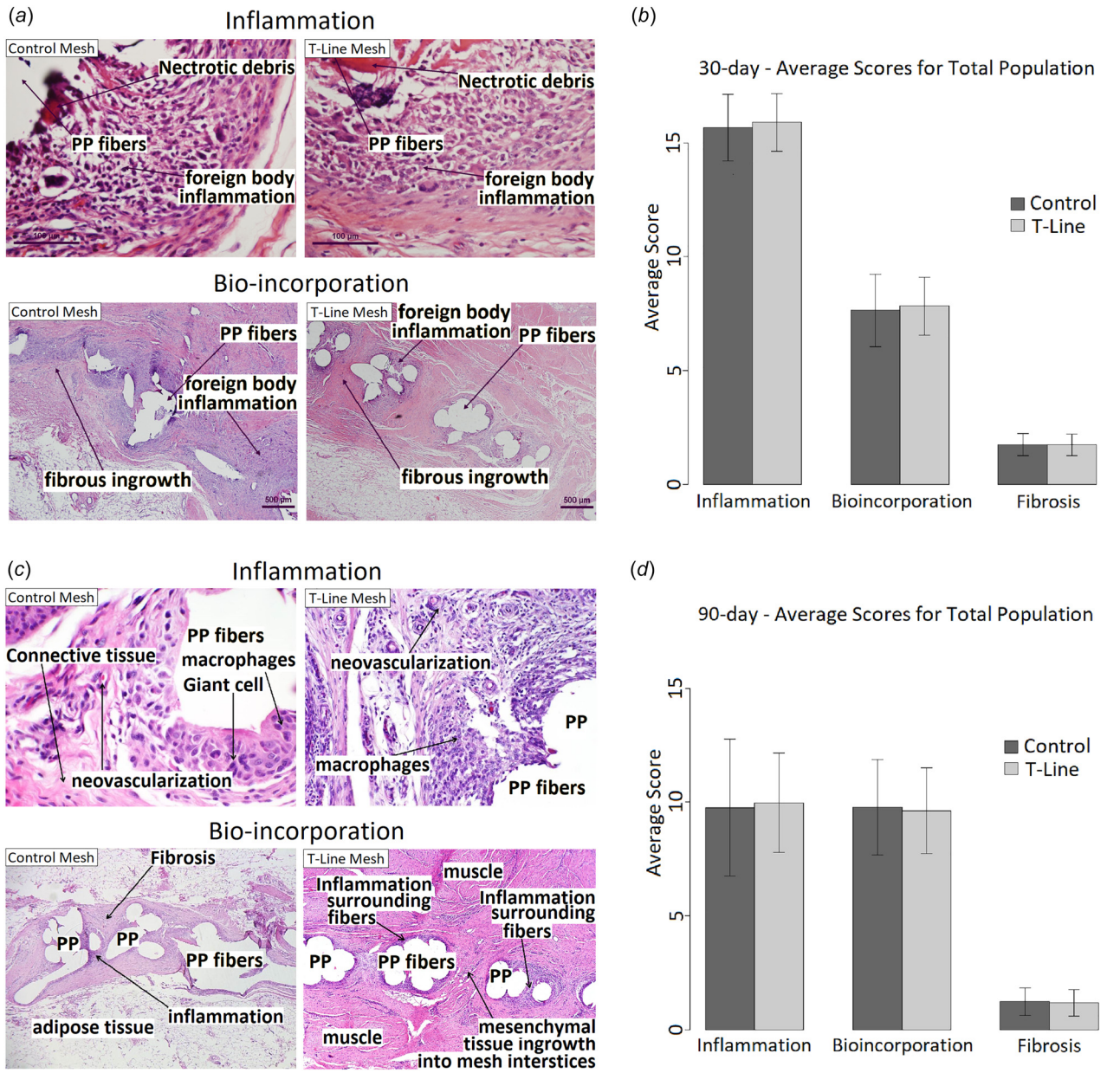

Fig. 5 Histological analysis of inflammation, bio-incorporation and fibrosis of the T-line and the predicate control mesh: microscopic images demonstrating inflammation and bio-incorporation after (*a*) 30 days and (*c*) 90 days. Quantification of the average scores of inflammation, bio-incorporation and fibrosis of the T-line mesh, and the control predicate mesh after (*b*) 30 days and (*d*) 90 days. There was no statistically significant difference between T-line and control mesh ($P > 0.05$).

to enhance inflammation because of the density of the mesh in the knot; although, SOC meshes are also known to cause intestinal adhesions so it is difficult to derive definitive conclusions. There are other approaches to securing an extension besides using a standard loop-on-end surgeon knot followed by three throws. We are currently developing these approaches to eliminate the need for a knot [32].

There are a few limitations to our study. First, we only tested anchor strength of 1.1 cm extensions. While the anchor strength was robust, it is possible that a narrower extension could achieve the same supraphysiologic, anchor point strength [28]. This could be advantageous because it would decrease trauma to the tissues through which it was passed. Second, we limited our application of mesh to the onlay position and did not test other application methods such as, retrorectus and underlay [33]. The reason why we only tested onlay was because this approach is simple to perform and widely practiced. Of course, the T-line mesh could also be applied as a retrorectus repair and underlay, and we are currently developing these approaches. Another weakness is that we investigated the repair in a clean wound and did not test the T-line mesh in an infected hernia model. While there is an increasing trend toward using permanent synthetic mesh in contaminated wounds, appropriate in vivo studies would need to be performed [34]. In this study, we also only compared the T-line mesh to suture anchoring of predicate mesh and did not study other anchoring methods such as glues, tacks, and screws. Lastly, we did not test the effects of cyclic stress or torsion stress on device performance. These stresses are commonly encountered from patient twisting and repeated bouts of coughing or straining and could be important to measure. Cyclic strain leads to micro tears which may summate to affect device performance [35].

5 Conclusion

The novel T-line mesh is a polypropylene, macroporous, moderate-weight mesh that meets all FDA standards and

outperforms a predicate mesh in each of the described mechanical performance tests. The T-line mesh is 275% stronger than SOC in the immediate postoperative period when anchor strength is needed most. There is no difference in inflammation, bioincorporation, and fibrosis between the T-line mesh and the predicate mesh. The T-line mesh has the potential to dramatically reduce hernia occurrence and recurrence.

Acknowledgment

The authors would like to thank Dr. Bruce Klitzman for his assistance and continuous support. The authors would like to thank Julie Fuller for her technical assistance with tissue processing. Thanks goes to the Secant Group (Telford, PA) for carrying out the physical and mechanical characterization of both the predicate mesh and experimental mesh.

Dr. Levinson is a founder of Deep Blue Medical Advances Inc. (DBMA) which has licensed the technology from Duke University. Dr. Ruppert is employed by DBMA and is an equity stakeholder.

Funding Data

- National Institutes of Health (NIH) (Grant Nos. 1 R41 GM117657-01 and 4 UL1TR001117-04; Funder ID: 10.13039/100000002).
- NC Biotechnology Center Technology Enhancement Grant (Funder ID: 10.13039/100005562).
- MedBlue (MedBlue Translational Grant).
- NC Biotechnology Center Small Business Research Loan (Funder ID: 10.13039/100005562).

References

[1] George, C. D., and Ellis, H., 1986, "The Results of Incisional Hernia Repair: A Twelve Year Review," Ann. R. Coll. Surg. Engl., **68**(4), pp. 185–187.
[2] Lamont, P. M., and Ellis, H., 1988, "Incisional Hernia in Re-Opened Abdominal Incisions: An Overlooked Risk Factor," Br. J. Surg., **75**(4), pp. 374–376.
[3] Luijendijk, R. W., Hop, W. C., van den Tol, M. P., de Lange, D. C., Braaksma, M. M., IJzermans, J. N., Boelhouwer, R. U., de Vries, B. C., Salu, M. K., Wereldsma, J. C., Bruijninckx, C. M., and Jeekel, J., 2000, "A Comparison of Suture Repair With Mesh Repair for Incisional Hernia," N. Engl. J. Med., **343**(6), pp. 392–398.
[4] Fischer, J. D., and Turner, F. W., 1974, "Abdominal Incisional Hernias: A Ten-Year Review," Can. J. Surg., **17**(4), pp. 202–204.
[5] Hesselink, V. J., Luijendijk, R. W., de Wilt, J. H., Heide, R., and Jeekel, J., 1993, "An Evaluation of Risk Factors in Incisional Hernia Recurrence," Surg. Gynecol. Obstet., **176**(3), pp. 228–234.
[6] Korenkov, M., Sauerland, S., Arndt, M., Bograd, L., Neugebauer, E. A., and Troidl, H., 2002, "Randomized Clinical Trial of Suture Repair, Polypropylene Mesh or Autodermal Hernioplasty for Incisional Hernia," Br. J. Surg., **89**(1), pp. 50–56.
[7] Read, R. C., and Yoder, G., 1989, "Recent Trends in the Management of Incisional Herniation," Arch. Surg., **124**(4), pp. 485–488.
[8] Richards, P. C., Balch, C. M., and Aldrete, J. S., 1983, "Abdominal Wound Closure. A Randomized Prospective Study of 571 Patients Comparing Continuous Vs. Interrupted Suture Techniques," Ann. Surg., **197**(2), pp. 238–243.
[9] Carlson, M. A., 1997, "Acute Wound Failure," Surg. Clin. North Am., **77**(3), pp. 607–636.
[10] Bhangu, A., Nepogodiev, D., and Futaba, K., West Midlands Research Collaborative, 2012, "Systematic Review and Meta-Analysis of the Incidence of Incisional Hernia at the Site of Stoma Closure," World J. Surg., **36**(5), pp. 973–83.
[11] Le Huu Nho, R., Mege, D., Ouaïssi, M., Sielezneff, I., and Sastre, B., 2012, "Incidence and Prevention of Ventral Incisional Hernia," J. Visc. Surg., **149**(5), pp. e3–e14.
[12] Pauli, E. M., and Rosen, M. J., 2013, "Open Ventral Hernia Repair With Component Separation," Surg. Clin. North Am., **93**(5), pp. 1111–1133.
[13] Sanders, D. L., and Kingsnorth, A. N., 2012, "The Modern Management of Incisional Hernias," BMJ, **344** (1), p. e2843.
[14] Wechter, M. E., Pearlman, M. D., and Hartmann, K. E., 2005, "Reclosure of the Disrupted Laparotomy Wound: A Systematic Review," Obstet. Gynecol., **106**(2), pp. 376–383.
[15] Brown, C. N., and Finch, J. G., 2010, "Which Mesh for Hernia Repair?," Ann. R. Coll. Surg. Engl., **92**(4), pp. 272–278.
[16] Cobb, W. S., Peindl, R. M., Zerey, M., Carbonell, A. M., and Heniford, B. T., 2009, "Mesh Terminology 101," Hernia, **13**(1), pp. 1–6.
[17] Klinge, U., Klosterhalfen, B., Conze, J., Limberg, W., Obolenski, B., Ottinger, A. P., and Schumpelick, V., 2003, "Modified Mesh for Hernia Repair That Is Adapted to the Physiology of the Abdominal Wall," Eur. J. Surg., **164**(12), pp. 951–960.
[18] Junge, K., Klinge, U., Prescher, A., Giboni, P., Niewiera, M., and Schumpelick, V., 2001, "Elasticity of the Anterior Abdominal Wall and Impact for Reparation of Incisional Hernias Using Mesh Implants," Hernia, **5**(3), pp. 113–118.
[19] Klinge, U., Conze, J., Limberg, W., Brücker, C., Ottinger, A. P., and Schumpelick, V., 1996, "Pathophysiology of the Abdominal Wall," Chirurg, **67**(3), pp. 229–233.
[20] Melman, L., Jenkins, E. D., Hamilton, N. A., Bender, L. C., Brodt, M. D., Deeken, C. R., Greco, S. C., Frisella, M. M., and Matthews, B. D., 2011, "Histologic and Biomechanical Evaluation of a Novel Macroporous Polytetrafluoroethylene Knit Mesh Compared to Lightweight and Heavyweight Polypropylene Mesh in a Porcine Model of Ventral Incisional Hernia Repair," Hernia, **15**(4), pp. 423–431.
[21] Lintin, L. A. D., and Kingsnorth, A. N., 2014, "Mechanical Failure of a Lightweight Polypropylene Mesh," Hernia, **18**(1), pp. 131–133.
[22] Souza, J. M., Dumanian, Z. P., Gurjala, A. N., and Dumanian, G. A., 2015, "In Vivo Evaluation of a Novel Mesh Suture Design for Abdominal Wall Closure," Plast. Reconstr. Surg., **135**(2), pp. 322e–330e.
[23] Lanier, A. T., Dumanian, G. A., Jordan, S. W., Miller, K. R., Ali, N. A., and Stock, S. R., 2016, "Mesh Sutured Repairs of Abdominal Wall Defects," Plast. Reconstr. Surg. Glob. Open, **4**(9), p. e1060.
[24] Tang, J. B., Amadio, P. C., Boyer, M. I., Savage, R., Zhao, C., Sandow, M., Lee, S. K., and Wolfe, S. W., 2013, "Current Practice of Primary Flexor Tendon Repair a Global View," Hand Clin., **29**(2), pp. 179–189.
[25] Earle, D. B., and Mark, L. A., 2008, "Prosthetic Material in Inguinal Hernia Repair: How Do I Choose?," Surg. Clin. North Am., **88**(1), pp. 179–201.
[26] Valentin, J. E., Badylak, J. S., McCabe, G. P., and Badylak, S. F., 2006, "Extracellular Matrix Bioscaffolds for Orthopaedic Applications. A Comparative Histologic Study," J. Bone Jt. Surg. Am., **8**(12), pp. 2673–2686.
[27] Deeken, C. R., Abdo, M. S., Frisella, M. M., and Matthews, B. D., 2011, "Physicomechanical Evaluation of Polypropylene, Polyester, and Polytetrafluoroethylene Meshes for Inguinal Hernia Repair," J. Am. Coll. Surg., **212**(1), pp. 68–79.
[28] Ibrahim, M. M., Poveromo, L. P., Glisson, R. R., Cornejo, A., Farjat, A. E., Gall, K., and Levinson, H., 2018, "Modifying Hernia Mesh Design to Improve Device Mechanical Performance and Promote Tension-Free Repair," J. Biomech., **71**, pp. 43–51.
[29] DuBay, D. A., Wang, X., Adamson, B., Kuzon, W. M., Jr. Dennis, R. G., and Franz, M. G., 2006, "Mesh Incisional Herniorrhaphy Increases Abdominal Wall Elastic Properties: A Mechanism for Decreased Hernia Recurrences in Comparison With Suture Repair," Surgery, **140**(1), pp. 14–24.
[30] Cassar, K., and Munro, A., 2002, "Surgical Treatment of Incisional Hernia," Br. J. Surg., **89**(5), pp. 534–545.
[31] Eriksson, A., Rosenberg, J., and Bisgaard, T., 2014, "Surgical Treatment for Giant Incisional Hernia: A Qualitative Systematic Review," Hernia, **18**(1), pp. 31–38.
[32] Green, J. L., Glisson, R., Hung, J., Ibrahim, M., Farjat, A., Liu, B., Gall, K., and Levinson, H., 2018, "Creating a Small Anchor to Eliminate Large Knots in Mesh and Tape Suture," ASME J. Med. Device, **12**(3), p. 035001.
[33] Jones, C. S., Nowers, J., Watts, A., Smart, N. J., and Daniels, I. R., 2017, "Incisional Hernia Repair With Retrorectus Synthetic Mesh and Abdominoplasty—A Video Vignette," Colorectal Dis., **19**(3), pp. 301–302.
[34] Petersen, L. F., McChesney, S. L., Daly, S. C., Millikan, K. W., Myers, J. A., and Luu, M. B., 2014, "Permanent Mesh Results in Long-Term Symptom Improvement and Patient Satisfaction Without Increasing Adverse Outcomes in Hiatal Hernia Repair," Am. J. Surg., **207**(3), pp. 445–448.
[35] Remache, D., Caliez, M., Gratton, M., and Dos Santos, S., 2018, "The Effects of Cyclic Tensile and Stress-Relaxation Tests on Porcine Skin," J. Mech. Behav. Biomed. Mater., **77**, pp. 242–249.